中國機械工程學刊第十九卷第二期第 231~236 頁（民國八十七年）
Journal of the Chinese Society of Mechanical Engineers, Vol.19, No.2, pp.231~236 (1998)

Research Note

Some Physical Insights Inside a Lid-Driven Rectangular Cavity

Te-Pu Chiang*, Robert R. Hwang** and Wen-Hann Sheu**

Keywords: Taylor-Görtler-like vortices, laminar instability.

ABSTRACT

A flow simulation is conducted to study the vortex structure in a three-dimensional rectangular cavity. The ratio of cavity depth to width is 1:1, and the span to width ratio is 3:1. The governing equations defined on staggered grids are solved in a transient context by using a finite volume method, in conjunction with a segregated solution algorithm. The focus of the present study is placed on the influence of the end walls on the evolving cavity flow physics. The flow dynamics of laminar instability is also discussed. To accomplish this task, the investigated Reynolds number is taken to be 1500.

INTRODUCTION

Recirculating flow is commonplace in many engineering practices. Conducting analyses to gain some insights into the evolution of vortical flows is, thus, critical for research scientists. An extensively studied lid-driven flow problem is investigated in this study. As shown in Fig.1, the rectangular cavity of the present interest possesses a depth to width ratio of 1:1, and a span to width ratio of 3:1. Geometric simplicity of the problem facilitates both experimental calibrations and numerical predictions.

From the knowledge gained from previous studies (Koseff and Street, 1984a; 1984b; Freitas et al., 1985; Freitas and Street, 1988; Aidun et al., 1991), it is now a generally recognized fact that the cavity of interest is filled with a primary eddy, two secondary eddies, and possibly several sets of meandering Taylor-Görtler-like (TGL) longitudinal vortices in cases when the Reynolds number is sufficiently high. Previous investigation, however, did not focus much on why TGL vortices burst in the flow. This motivates us to conduct this study with an aim to broaden our understanding of the mechanism leading to the laminar instability in the lid-driven cavity.

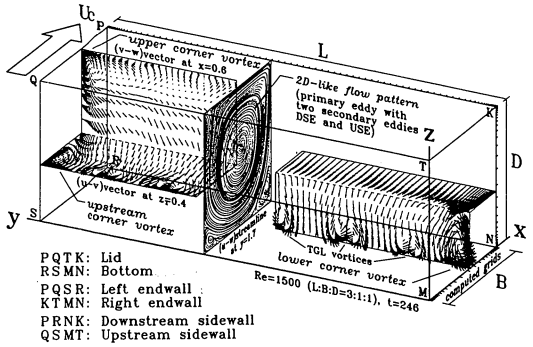

Fig.1. Geometric definition and the description of the flow structures.

GOVERNING EQUATIONS AND NUMERICAL PROCEDURES

We consider in this study the following dimensionless velocity-pressure formulation for an incompressible Navier-Stokes fluid flow:

$$\frac{\partial u_i}{\partial x_i} = 0, \tag{1}$$

$$\frac{\partial u_i}{\partial t} + \frac{\partial}{\partial x_m}(u_m u_i) = -\frac{\partial p}{\partial x_i} + \frac{1}{Re}\frac{\partial^2 u_i}{\partial x_m \partial x_m}, \tag{2}$$

where $i = 1 \sim 3$. Hereinafter, u_i and p are denoted as the velocity components and the modified pressure, respectively. In Eq.(2), $Re = \frac{U_c B}{\nu}$ is referred to as the Reynolds number, where ν stands for the kinematic

Paper Received June, 1997. Revised October, 1997. Accepted October, 1997. Author for Correspondence: Te-Pu Chiang.

* *Associate Professor, Department of Naval Architecture and Ocean Engineering, National Taiwan University, Taipei, Taiwan, ROC.*

** *Professor, Department of Naval Architecture and Ocean Engineering, National Taiwan University, Taipei, Taiwan, ROC.*

viscosity, B the width of the cavity, and U_c the lid velocity.

To avoid oscillatory pressures, the present analysis is formulated in the physical domain with staggered grids (Patankar, 1980). This grid arrangement facilitates conducting a finite volume integration of working equations in their representative control volume. In modeling the equations of motion, a higher-order QUICK scheme of Leonard (1979) has been chosen for discretizating non-linear advective fluxes. Amongst the possible solution algorithms to solve for primitive variables, we adopt the segregated approach, known as the SIMPLE solution algorithm (Patankar, 1980). The readers are referred to our earlier work (Chiang et al., 1996) providing a code validation study.

RESULTS AND DISCUSSION

For this study, solutions are obtained in a mesh of grid resolution by $34\times91\times34$. The grid is stretched in regions where boundary layers may develop. In the case of Re=1500, five sets of well-developed TGL vortices, as shown in Fig.1, are observed over the entire span. The same number of less apparent vortices are also visible on the upper ceiling lid plane. This flow is characterized as time-periodic with a periodicity of 72 (Chiang et al., 1996).

Flow Pattern at y Planes

In an attempt to address the importance of the two end-walls, we plotted sectional streamlines (i.e., pseudo-streamlines). These lines are obtained by integrating the (u, w) velocity components lying in the cut plane as given in Fig.2. Being influenced by the fluid viscosity, the circulating flow character in the region of $2.9 \leq y < 3$ differs from that in the rest of the half cavity. More precisely, the spanwise motion has little effect on the primary flow motion when $1.5 < y < 2.8$. Also, the centers of the primary vortices are seemingly invariant with the spanwise location.

Due to the presence of two end walls, the negative pressure gradient established along the spanwise direction results in inward-running motion in the core region of the primary cell. An outward-running motion is also observed in the outer region bounded by walls due to the continuity constrain. In support of the sign-switching of v, we also plotted dashed isolines of v=0 in Fig.2. Near the two end walls, it is tempting to say that pseudo-streamlines and contour lines of v=0 are seemingly irrelevant. This is a great aid in making room for the maintenance of flow stability. As the value of y decreases to 2.8, the degree of

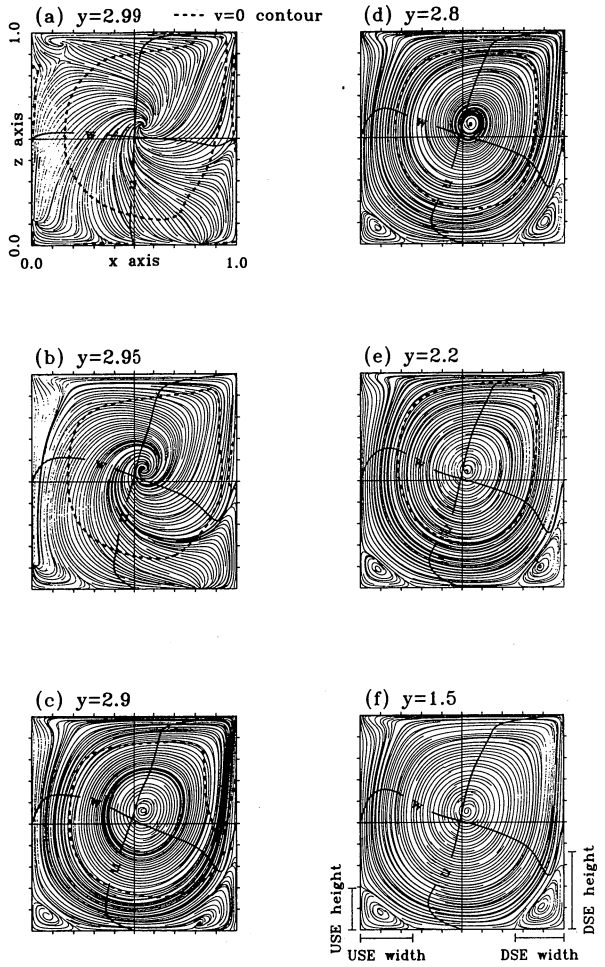

Fig.2. Descriptions of flow pattern at y planes by virtue of pseudo-streamlines at t=30. (a) y = 2.99; (b) y = 2.95; (c) y = 2.9; (d) y = 2.8; (e) y = 2.2; (f) y = 1.5.

resemblance between these two classes of lines keeps increasing. Also, the downstream secondary eddy (DSE) and the upstream secondary eddy (USE) are increasingly apparent. A close parallelism between pseudo-streamlines and isolines v=0 gives impetus to destabilization of the confined flow system.

Eddy Sizes of DSE and USE

The lengths defined in Fig.2(f) provide us with useful knowledge about the entry point from which fluid particles inside the DSE and USE can commute with those inside the core of the cavity. As seen in Fig.3, eddy sizes of DSE and USE at t = 30 vary over the span. In between y = 2.85 and y = 3, the height of the DSE increases while the width decreases. To the contrary, the width of the USE increases while

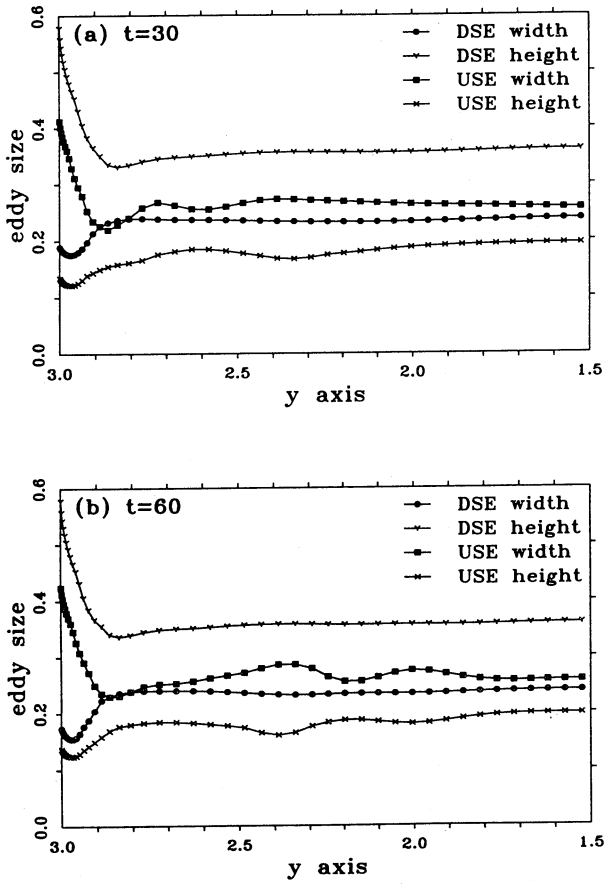

Fig.3. Eddy sizes (defined in Fig. 2) of DSE and USE along the span-wise direction. (a) $t = 30$; (b) $t = 60$.

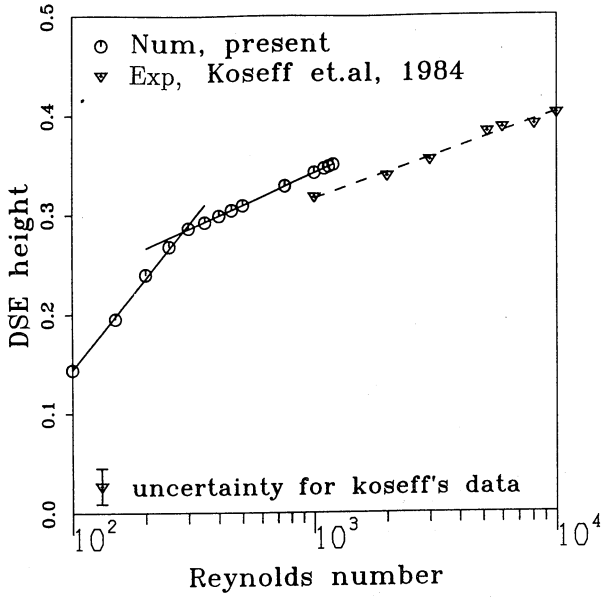

Fig.4. A comaprison study of the heights of DSE at different Reynolds numbers.

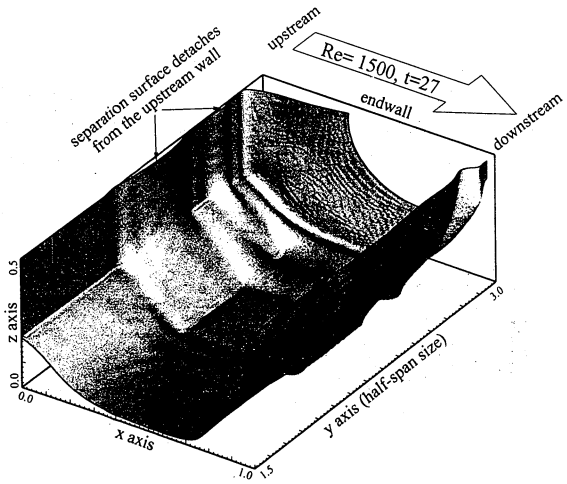

Fig.5. Separation surface (which separates the primary core from the USE and DSE) detaches from the upstream sidewall.

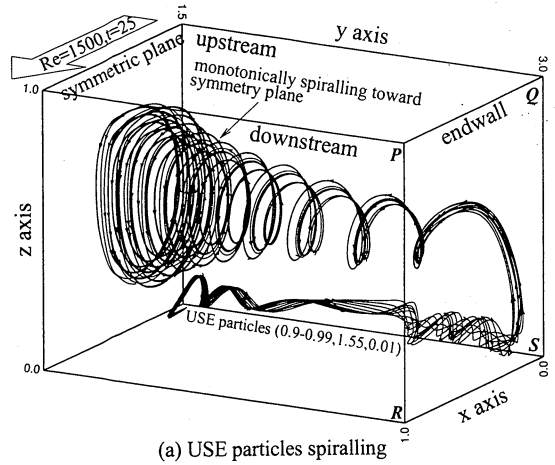

(a) USE particles spiralling

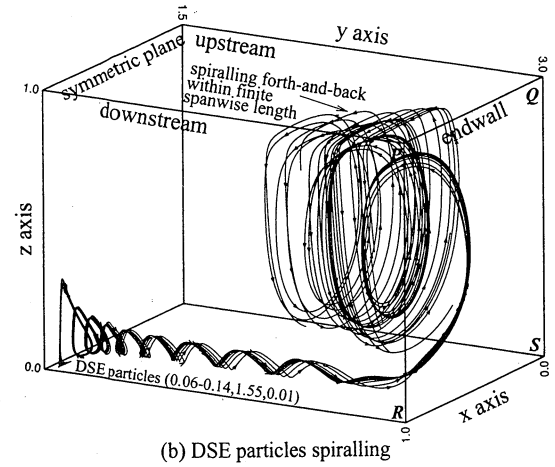

(b) DSE particles spiralling

Fig.6. Illustration of spiralling flow motion in a half-span cavity. (a) USE particles; (b) DSE particles;.

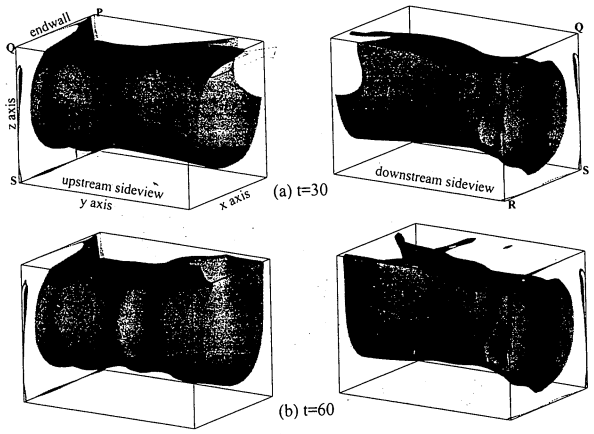

Fig.7. The perspective views of v=0 isosurface in a half-span cavity. (a) $t = 30$; (b) $t = 60$.

the height decreases. Before closing this section, it is worthwhile to compare the height of the DSE with that of the Koseff and Street (1984a; 1984b). Taking the experimental uncertainty, say 0.035 (Koseff and Street, 1984a; 1984b), into consideration, good agreement between the numerical result and the experimental data is demonstrated in Fig.4. The key observation from this figure is that the hight of DSE has a marked change at $Re = 300$. This is indicative of the flow which is prone to show three-dimensional characters. Figure 5 plots the surface which separates the primary circulating cell and the secondary eddies. It is this concave surface that induces a centrifugal force which tends to destabilize the flow system.

Spiral Vortex System

As a means of investigating the spiraling flow structure, we keep track particles which are originally released from some representative locations. In an attempt to demonstrate the distinct nature of the DSE and USE, we selected particles in the DSE and the other ones in the USE and then plotted their ensuing helixes in Fig.6. These constitute two of the three larger spiraling motions in the investigated enclosure. Being influenced by the aforementioned end-wall induced suction force, each helix under these circumstances is the result of the established pressure field. The released particles are, thus, dragged to two endwalls and are finally sucked into the primary core.

Figure 7 shows the the three-dimensional contours of the zero spanwise velocity. For particles inside this tube they move to the symmetry plane. The rest of fluid particles proceed in an opposite flow direction. Spiraling structure of this sort is an inevitable outcome of intriguing spanwise velocities be-

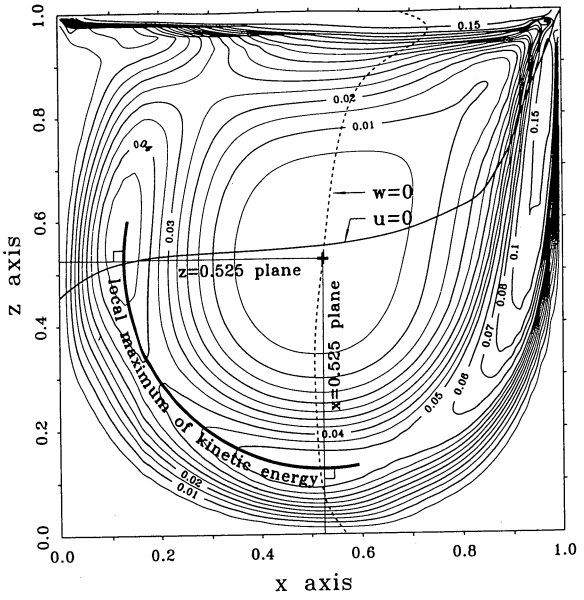

Fig.8. The contours of kinetic energy at the symmetry plane at t=30.

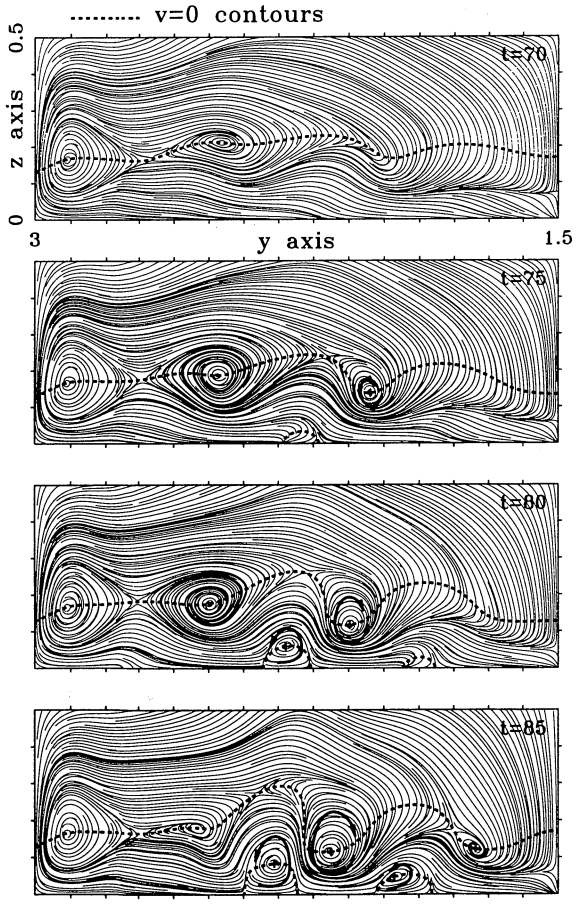

Fig.9. Formation of TGL vortices at x=0.525 plane.

cause fluid particles belonging to one spanwise plane will enter another parallel plane.

Longitudinal Instability

According to Fig.2, pseudo-streamlines increasingly parallel to the zero spanwise velocity contour surface at spans which are increasingly closer to the symmetry plane (x, y=1.5, z). Particles moving towards the symmetry plane are featured by having a monotonic spiraling motion. Newly revealed from the present study is that for particles at the USE they monotonically move towards the symmetry plane (Fig.6(a)); while for particles in the DSE they may move back and forth within a finite spanwise length (Fig.6(b)). Figure 6 reveals that the motion of fluid particles near the end wall (Fig.6(b)) is easier to satisfy the mass conservation by the nature forces via corner vortex; while for particles near the symmetry plane (Fig.6(a)) is hardly achievable. This implies the symmetry plane (in the presence of two end walls), serving as a destabilized means, causes the formation of the wave-like disturbance which propagates towards the two-end walls. This finding is in contrast to the pioneer work of Freitas and Street (1988) who claimed the EWCE (end wall corner eddy) induces a wave-like disturbance which propagates from the end wall.

On the increase of Reynolds number, the flow evolves from a steady state to its unsteady counterpart, followed by a time-periodic propagation and finally the emergence of TGL vortices. This is the main reason why the upstream side of the v=0 isotube, as shown in Fig.7(b), has been appreciably twisted. In contrast, the surface of v=0 is much smoother at the downstream side, similarly, Fig.3(b) provides a clear manifestation of variations of width and height for the USE. It is tempting to say that flow system in DSE is more stable than that in the USE.

Energy Aspect

It is worthwhile to point out where the onset of the disturbance will most likely occur at x and z planes. To answer this question, we plotted kinetic energy ($\equiv \frac{1}{2}(u^2 + v^2 + w^2)$) contours at the y=1.5 plane in Fig.8 and tracked their relative maximum at upstream side. This locus falls into a circle of radius 0.4, centered at (x=0.525, z=0.525). Kinetic energy drastically change their values either at the x=0.525 plane or at the z=0.525 plane. This implies that the largest centrifugal force renders the greatest possibile instability therein. As for other y planes, we can draw a conclusion similar to that obtained at the symmetry plane. With this rationale, we believe that the formation of TGL vortices are most clearly demonstrated at x=0.525 plane as shown in Fig.9. At a short distance from x=0.525, say at x=0.5 and x=0.55, the structure of TGL vortices is not visible at all, as shown in Fig.10.

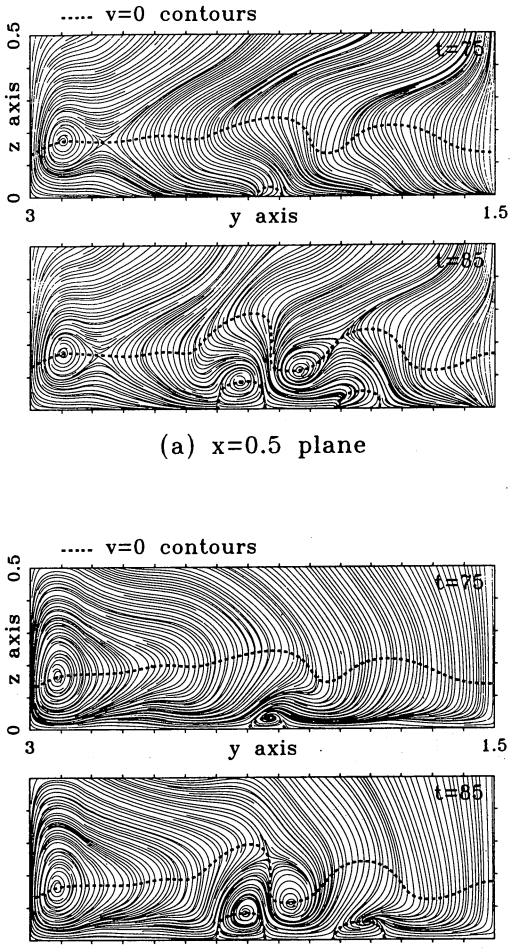

Fig.10. The structure of TGL vortices, especially the vortex generated along v=0 contour, is not visible in the x plane others than 0.525. (a) $x = 0.5$; (b) $x = 0.55$.

CONCLUSIONS

In the global context, we have concluded that the presence of inward-running primary vortices and two adjacent outward-running DSE and USE vortices manifest this spiraling system. In the local sense, there exist five sets of mobile Taylor-Görtler-like vortices and a pair of corner vortices in the vicinity of the end-walls. Fluid particles coming across corner

vortices will be quickly lifted up and are then drawn in the primary core. Of various locations at x and z planes, TGL vortices are clearly observed at x=0.525 and z=0.525 planes where the steepest change on the kinetic energy is revealed. This, in turn, yields a larger centrifugal force therein. In view of the protrusions emanating from the three-dimensional surface of v=0, together with an appreciable waviness in the eddy size, we believe that spiraling character inside USE destabilizes the flow system.

ACKNOWLEDGMENT

The authors would like to express their thanks for financial support from the National Science Council under contract number NSC 80-0410-E002-51.

REFERENCES

Aidun, C.K., Triantafillopoulos, N.G., and Benson, J.D., "Global Stability of a Lid-Driven Cavity with Throughflow: Flow Visualization Studies," *Phys. Fluids*, A3, pp.2081-2091 (1991).

Chiang, T.P., Hwang, R.R., and Sheu. W.H., "Finite Volume Analysis of Spiral Motion in a Rectangular Lid-Driven Cavity," *Int. J. Numer. Methods Fluids*, Vol.23, pp.325-346 (1996).

Freitas, C.J., Street, R.L., Findikakis, A.N., and Koseff, J.R., "Numerical Simulation of Three-Dimensional Flow in a Cavity," *Int. J. Numer. Methods Fluids*, Vol.5, pp.561-575 (1985).

Freitas, C.J., and Street, R.L., "Non-Linear Transport Phenomena in a Complex Recirculating Flow: A Numerical Investigation," *Int. J. Numer. Methods Fluids*, Vol.8, pp.769-802 (1988).

Koseff, J.R., and Street, R.L., "Visualization Studies of a Shear Driven Three-Dimensional Recirculating Flow," *ASME Journal of Fluids Engineering*, Vol.106, No.1, pp.21-29 (1984a).

Koseff, J.R., and Street, R.L., "On End Wall Effects in a Lid-Driven Cavity Flow," *ASME J. Fluids Engineering*, Vol.106, pp.385-389 (1984b)

Leonard, B.P., "A Stable and Accurate Convective Modeling Procedure Based on Quadratic Upstream Interpolation," *Comput. Methods Appl. Mech. Engrg.*, Vol.19, pp.59-98 (1979).

Patankar, S.V., *Numerical Heat Transfer and Fluid Flow*, Hemisphere (1980).

頂板曳動穴流場之若干物理現象探源

蔣德普　黃榮鑑　許文翰

國立臺灣大學造船及海洋工程學系

摘　要

本文進行流場數值模擬，探討幾何尺度比為 3:1:1 之三維頂板曳動穴流場中的渦旋結構；數值程序係於交錯佈置網格中，循序求解經有限體積法離散之時變性流場控制方程式。研究的重心在於物理性地闡述：主流方向之側壁面於引發三維層流不穩定機制中所扮演的角色，流場雷諾數為 1500。